

1 Revisiting the Sunspot Number as EUV proxy for ionospheric F2 critical frequency

2
3 Bruno S. Zossi^{1,2}, Franco D. Medina^{1,2}, Trinidad Duran^{3,4}, Blas F. de Haro Barbas^{1,2} and Ana G. Elias^{1,2}

4 (1) Laboratorio de Ionosfera, Atmosfera Neutra y Magnetosfera (LIANM), Facultad de Ciencias
5 Exactas y Tecnología (FACET), Universidad Nacional de Tucumán (UNT), Argentina

6 (2) INFINOA, CONICET-UNT, Argentina

7 (3) Departamento de Física, Universidad Nacional del Sur (UNS), Bahía Blanca, 8000, Argentina

8 (4) Instituto de Física del Sur (CONICET-UNS), Bahía Blanca, 8000, Argentina

9 10 **Abstract:**

11 This study reconsiders the Sunspot Number (Sn) as a solar extreme ultraviolet (EUV) proxy for
12 modeling the ionospheric F2 layer's critical frequency (foF2) over the period 1960-2023. We
13 compare the performance of Sn with F10.7 and F30 solar radio fluxes, focusing on their ability to
14 model the Global Ionospheric index (IG). Our results reveal that while F30 has shown a better
15 correlation in recent solar cycles, the Sn is the most stable and reliable over the entire dataset,
16 obtaining the highest correlation. In addition, if we remove the saturation effects from the
17 considering a maximum value of Sn, the correlation increases, outperforming all other proxies, and
18 predicting correctly the long-term trend estimated by general circulation models.

19 **Plain Language Summary**

20 The Earth's ionosphere, a critical layer for radio communication and GPS signals, is influenced by the
21 Sun's radiation. To understand how the ionosphere changes over time, scientists use measurements
22 of solar activity called proxies. In this study, different proxies are evaluated to find the best one for
23 modeling ionospheric conditions over the last 60 years. Despite being an older measure, we found
24 that the Sunspot Number is the most reliable for long-term studies, outperforming newer proxies in
25 some cases. Our work suggests that relying on newer proxies might lead to inaccurate predictions,
26 especially during periods of low solar activity.

27 28 **Key Points**

- 29 • The Sunspot Number (Sn) outperforms F30 and F10.7 solar proxies in long-term ionospheric
30 datasets, especially before 1980 and during recent solar cycles.
- 31 • Removing the saturation effect from the Sn dataset further enhances its correlation with
32 the Global Ionospheric index (IG), improving long-term trend predictions.
- 33 • The study emphasizes the variable performance of solar proxies over time, with Sn showing
34 the greatest stability for modeling ionospheric conditions across six decades.

35 36 **1. Introduction:**

37 The understanding of atmospheric trends became a critical area of study in the last century. Besides
38 the troposphere, the upper atmosphere is also affected by human activities. Many modern
39 technologies, such as long-distance telecommunications, global positioning systems (GPS), and
40 satellite communications, rely on space and near-Earth physics (Zolesi and Cander, 2014). One
41 important part of the upper atmosphere is the ionosphere, defined as the zone where the presence
42 of free charges is high enough to affect the propagation of electromagnetic waves. Long-term trends
43 in this region arise primarily from the greenhouse effect but are also influenced by long-term solar
44 periodicities and the secular variation of Earth's magnetic field (Lastovicka, 2023).

45 This ionized area is mainly affected by solar extreme ultraviolet radiation (EUV), which is absorbed
46 by the neutral components, heating and ionizing them. To model this atmospheric layer, direct
47 measurements of EUV are needed. However, such data have only been available since the satellite
48 era, therefore, several models were developed using EUV proxies, or, different measurements that
49 are closely linked to the needed variable (Bilitza et al. 2022, Liu et al. 2010). Modern proxies measure
50 solar irradiance at specific wavelengths in satellites, avoiding the interaction with the atmosphere.
51 The most common are magnesium II wing-to-core ratio, helium II, and Lyman-alpha, among others.

52 The ionospheric structure has been measured since the 1930s after the development of the
53 ionosonde. This instrument operates by emitting a vertical electromagnetic wave from the ground
54 and waiting for the reflection of the wave. The internal layers are reached using different
55 frequencies. The ionosphere is mainly studied through ionosonde databases, mainly due to their
56 long period and the reliability of the available data. The main data produced by ionosondes are the
57 critical frequencies and the peak height of each layer.

58 Over the past decades, various solar indices have been employed as proxies for estimating
59 ionospheric parameters. Among these, the S_n has historically been one of the most reliable proxies
60 due to its long record and strong correlation with solar EUV radiation, which directly affects the
61 ionosphere. However, newer solar indices, such as the F10.7 cm solar radio flux (Lastovicka et al.
62 2006, Mielich and Bremer (2013), Jakowski et al. 2024), and the more recent F30 (Lastovicka 2021,
63 Dudok de Wit and Bruinsma 2017, Zossi et al. 2024), as well as MgII (de Haro Barbas et al. 2021),
64 have been introduced as alternatives that may offer better correlations under specific conditions or
65 periods.

66 Recent studies have debated the effectiveness of these proxies, particularly in representing
67 ionospheric trends during periods of low solar activity, such as the deep minima of solar cycles 24
68 and 25. These discussions have highlighted the need for continuous evaluation of solar proxies to
69 ensure accurate long-term trend predictions, which are crucial for both scientific understanding and
70 practical applications in space weather forecasting.

71 In recent years, some articles studied the changes in the relationship between the sunspot number
72 and the solar radio fluxes, identifying a trend associated with the Sun that affects this relationship
73 (Clette 2021, Mursula et al. 2022, 2024). The solar radio fluxes trend to increase compared to the
74 sunspot number, this trend may introduce an error in models, which rely on these indices.

75 In this study, we assess the performance of the S_n , F10.7, and F30 as proxies for modeling
76 ionospheric foF2 for the period 1960-2023, particularly focusing on their ability to model the
77 ionospheric index IG, a key indicator of global ionospheric conditions. We examine the stability and
78 correlation of these proxies over different solar cycles and discuss the implications of choosing one

79 proxy over another for long-term ionospheric studies. This procedure results in a better
80 performance of Sn over F10.7 and F30 to reproduce the complete IG dataset, mainly during the
81 complicated solar cycles 20, 23, and 24.

82

83 **2. Data**

84 The foF2 monthly median time series used in this work are from the following 10 stations: Wakkanai
85 (45.2°N, 141.4°E), Kokubunji (35.7°N, 139.5°E), Okinawa (26.3°N, 127.6°E), Hobart (42.5°S, 147.2°E),
86 Canberra (35.2°S, 149.1°E), Townsville (19.2°S, 146.5°E), Sodankyla (67.3°N, 26.3°E), Boulder
87 (40.1°N, 105.2°W), Juliusruh (54.6°N, 13.4°E), and Rome (41.5°N, 12.3°E). The selected stations have
88 long records, covering, in some cases, more than 60 years. Due to the uncertainties and bad reading,
89 some data were discarded. The criteria used to calculate the monthly medians for each hour re-
90 quired at least 15 days available with measurements in every month, and checking outliers in every
91 case. Most of the datasets were extracted from Damboldt and Suessmann database (Damboldt and
92 Suessman 2012). The data was updated until 2022 using records from Lowell GIRO Data Center
93 (LGDC) (Reinisch and Galkin 2011). foF2 from the Digital Ionogram Data Base (DIDBase) at LGDC has
94 a frequency of 5 to 15 minutes. To obtain the monthly medians, data with Autoscaling Confidence
95 Score (CS) greater than 60% was first selected, and then the hourly median for each month was
96 estimated. We checked that the last two years available from Damboldt and Suessman database
97 had a reasonable coincidence (within 5%) with the data obtained from GIRO.

98 In this work, the Global Ionospheric index (IG) is used to analyze the solar proxies. IG was originally
99 computed using 13 globally distributed ionosonde stations. The distribution of these stations was a
100 compromise between good global coverage and reliable long-operating-period ionosonde stations.
101 However, due to station closures and data unavailability, the number of stations used in IG has
102 decreased to four (Brown et al., 2018). Therefore, since IG is derived from ionospheric
103 measurements, it captures foF2 variations not driven solely by solar activity, such as those caused
104 by increased greenhouse gases.

105

106 **3. Methodology**

107 In this work, we use linear regressions between the annual averaged IG index, which represents
108 ionospheric foF2, and solar proxies. The linear regression is a simple statistical method that models
109 the relation between two variables using a linear equation,

$$110 \quad y = \alpha_0 + \alpha_1 x \quad (1)$$

111 where α parameters are the regression coefficients, usually estimated using least squares, and \mathbf{x}
112 and \mathbf{y} are the independent and dependent variables, respectively.

113 This regression is widely used for systems highly sensitive to a given variable or parameter. For
114 example, many upper atmosphere parameters, when dealing with annual means, respond to the
115 solar flux almost linearly. We also extend to a second-order regression, which is the same procedure,
116 but adding a squared term of variable x .

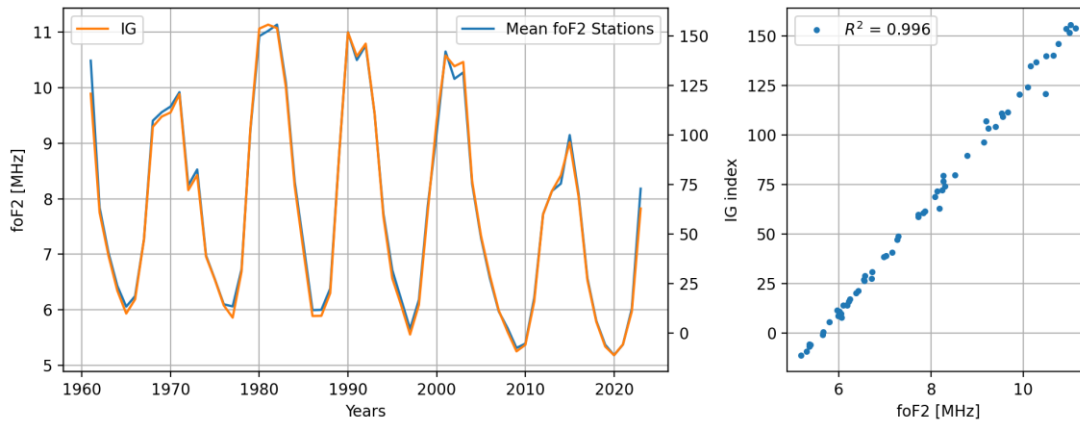
117 To compare the performance of each proxy we use the squared correlation coefficient, R^2 , which
118 provides a measure of the variance of y predicted by the model using the independent variables.

119

120 4. Results and Discussion

121 Using IG index as a global mean ionospheric condition. IG values are scaled to sunspot number, it
122 represents foF2 from different stations around the world. Figure 1 shows the yearly averaged values
123 of foF2 for the stations used in this work and the IG index, the correlation between both is also
124 plotted. With an R^2 of 99.6%, we can say that the IG index is a reliable representation of ionospheric
125 conditions. Therefore, we will use it to compare with the solar EUV proxies.

126



127

128 Figure 1. Yearly noon mean (12 LT) foF2 for the ten stations used in this work (blue), and IG index
129 (orange). The right panel shows the linear correlation between IG and foF2, the explained variance
130 $R^2 = 0.996$.

131

132 The variability of ionospheric foF2, at the interannual scale, is mainly driven by solar activity. For this
133 reason, many (practically any) EUV proxies result in an excellent correlation with annual averaged
134 foF2.

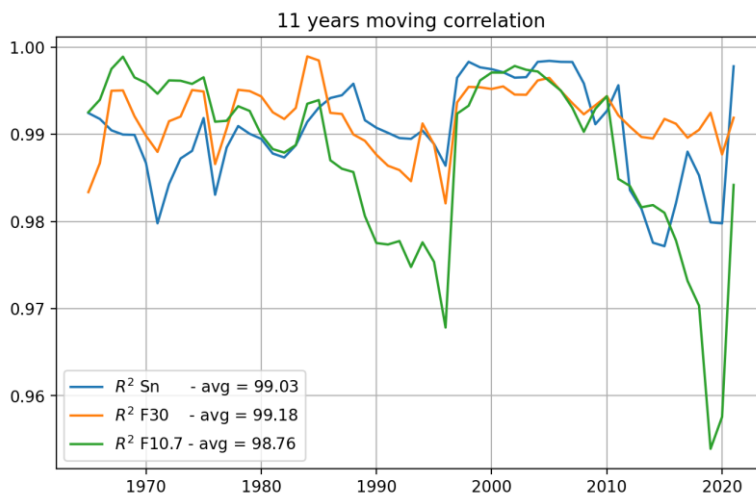
135 As we mentioned, in the last years, many articles have been published trying to find the correct
136 proxy for long-term trend estimation. Historically, the more used were the oldest, the sunspot
137 number, and the solar fluxes at radio wavelengths, having measured datasets of 70 years and more.
138 However, such long datasets for ionospheric conditions are uncommon, just a bunch of measuring
139 stations have reliable data in this period.

140 Lastovicka (2021) criteria for selecting the best solar proxy include the high correlation, temporal
141 stability, and, the trend estimation having a consistent sign throughout the entire period. Based on
142 these factors, the study concluded that F30 is the most suitable EUV proxy for ionospheric long-term
143 trend estimation. The trend estimation is compared to general circulation models (Solomon et al.
144 2018), where the solar activity remains constant while greenhouse gases increase, resulting in a
145 trend of $\sim -0.6\%$ /decade for foF2.

146 As the main issue is to find long ionospheric datasets, in many articles, the trends are often assessed
147 using data up to 2008, avoiding the deep solar minimum, or from 1985 to the present. The important
148 historical issues were the correlation decreasing in some periods and the change in the estimated

149 trend after filtering the solar activity. These problems turn into the necessity of looking for other
150 solar EUV proxies, particularly given the unique characteristics of the last solar cycles 24 and 25,
151 which featured two deep minima with prolonged periods of zero sunspot numbers. During these
152 deep minima, the ionospheric foF2 drops below historical minimum values, this fact can be easily
153 noted since the IG index takes the most quantity of negative values in the last two cycles.

154 The stability of the correlation between proxies and data results in a slight average correlation of
155 F30 over Sn and F10.7. This can be seen in Figure 2, where an 11-year centered moving correlation
156 was calculated between IG and the three proxies. F10.7 shows two periods of lower correlation, this
157 is a key reason for the need to use another proxy. On average, F30 has a higher correlation using
158 this comparative analysis, especially in the last cycle, where correlations for the other proxies
159 decrease. Sn has a step down in this last cycle but is the best from 1990 to 2008 approximately,
160 where solar fluxes have a noticeable correlation decrease.



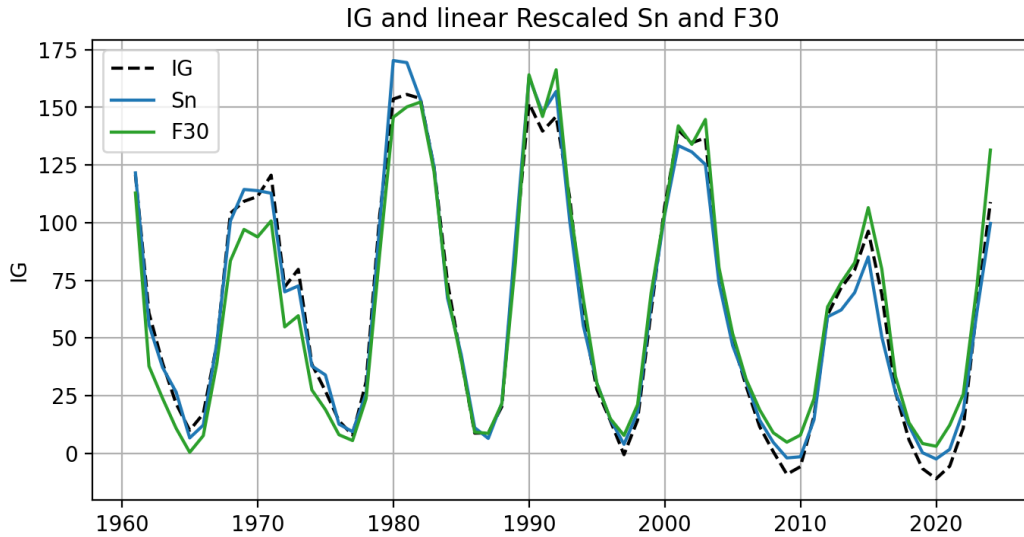
161

162 Figure 2. 11-year moving squared linear correlation between IG and solar EUV proxies: Sn (blue),
163 F30 (orange), and F10.7 (green).

164

165 The linear correlation analysis indicates that Sn and F30 are better reproducing the variability of
166 foF2, through the IG index. Figure 3 shows the IG values modeled linearly using both proxies along
167 with the original dataset. This figure helps to contextualize the moving correlation seen in Figure 2.
168 In all maximums after 1980, F30 is closer to IG values, however, in the complete previous solar cycle;
169 Sn models better the ionospheric index. On the other hand, during minimum solar periods, Sn
170 outperforms F30, even during the last two deep minimum cycles. Taking into account that Sn has a
171 minimum possible value of zero, is expected to fail to reproduce these last two cycles, however, F30
172 does not reproduce the IG index decrease.

173



174

175 Figure 3. Linear modeling of the ionospheric IG index using F30 (green) and Sn (blue), with the
 176 observed IG index (black dashed line).

177

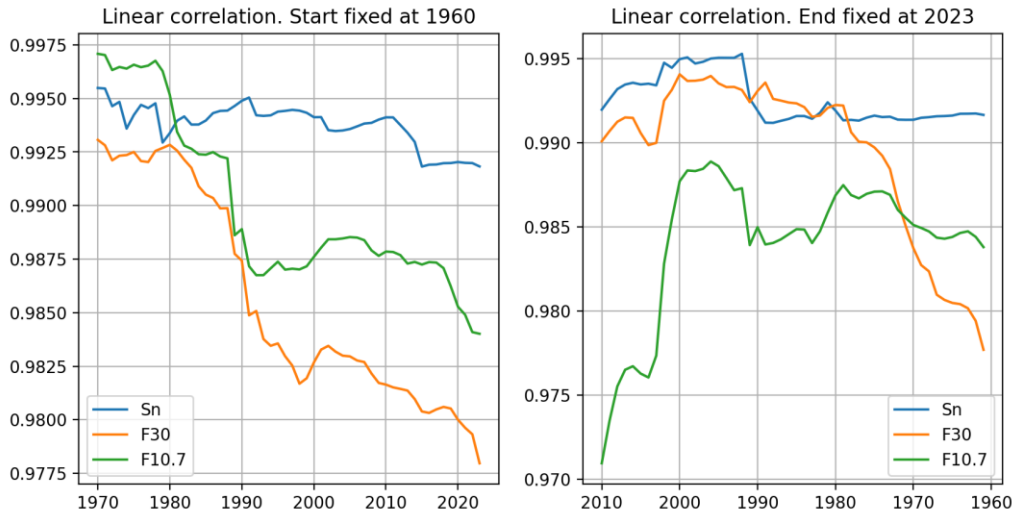
178 There is a clear trend between Sn and F30, note in Figure 3 how F30 (green line) is under the Sn
 179 (blue line) up to ~1990, where two lines cross, and after this time, F30 models higher values of IG at
 180 almost every point. This behavior is closely linked to the analysis made by Mursula et al. (2024); they
 181 compare the solar flux indices with the sunspot number, identifying this increasing trend.

182 At this point, an important problem arises, if solar fluxes increase compared to IG, which represents
 183 ionospheric foF2 level, we can anticipate a decreasing trend in the residuals if we subtract IG
 184 modeled with F30 from the original data. Perhaps, looking for a proxy with a decreasing trend led
 185 us to a mistake with F30, mainly, taking into account that F30 do not obtain the highest correlation
 186 before ~1980.

187 This can be noted in Figure 4, where we perform an ending point moving correlation, fixing the first
 188 year in 1960, changing the last year, and calculating the linear correlation of IG and the three
 189 proxies. Additionally, the same analysis is performed in reverse, fixing the final year at 2023,
 190 changing the first year, and estimating the linear correlation. In Figure 4, the superior performance
 191 of Sn to predict IG is clear, the left panel shows that starting the analysis in 1960, Sn is the best in
 192 almost the complete period, except for F10.7 at the beginning. On the other hand, the right panel
 193 explains why F30 is sometimes considered the best, fixing the last year and adding years backward
 194 in time, can be noted that, if the correlation analysis begins in the period 1980-1990, F30 is the best,
 195 but looking the complete panel, is clear that is just for that period. This is clearer comparing with
 196 Figure 3, where we noted that F30 fails to model the beginning and the end of the IG dataset.
 197 Moreover, Sn has a clear higher stability in this kind of analysis, therefore, the question is, why are
 198 we discarding Sn as a solar EUV proxy?

199 Note that the analysis of Figure 4 is completely different from the result of Figure 2, due to the
 200 variation in the initial and ending years, the result of the best correlation using F30 can be obtained

201 reducing the period used in the correlation. This discrepancy is associated with the inclusion, or not,
202 of solar cycle 20 (1964-1976), where F30 does not represent properly the IG index variability.

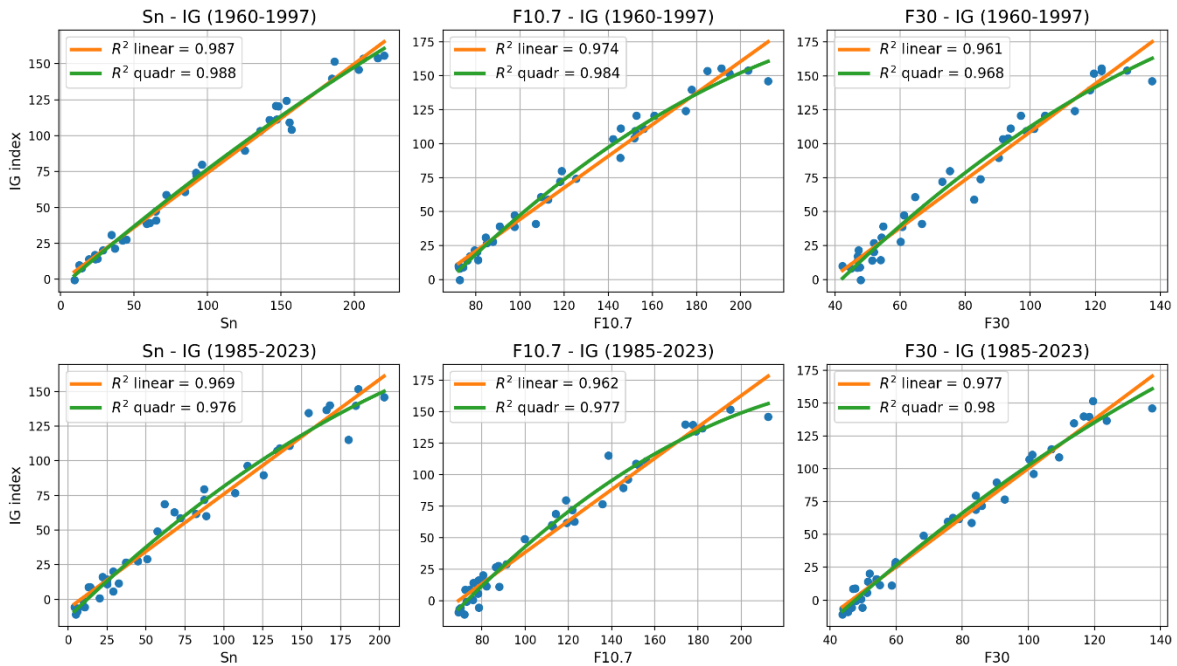


203
204 Figure 4. Squared linear correlation between IG and Sn, F30 and F10.7 with moving end year (left),
205 and inverse, moving start year (right).

206

207 An important ionospheric feature is the saturation (Balan et al., 1994; Liu et al., 2003). During the
208 daytime, there is a maximum possible value of foF2, even if solar flux continues increasing. This
209 problem is more evident at shorter time scales. Many authors deal with this by performing a
210 quadratic and even cubic regression between proxies and foF2 (Liu et al., 2006; Ma et al., 2009;
211 Danilov and Berbeneva, 2023). However, this effect is not that clear when analyzing annual means.
212 Figure 5 shows the linear and quadratic regression between proxies and IG separately for periods
213 1960-1997, and 1985-2023, to have the same number of years in each regression. Again, we can
214 mention the higher performance of Sn in the first cycles, and F10.7 is the second-best proxy. In
215 contrast, F30 obtains a higher correlation in the second period. There is a weak improvement using
216 quadratic regression at the annual scale, this can be noticed in each panel. The F10.7 exhibits a more
217 significant increase in the correlation.

218

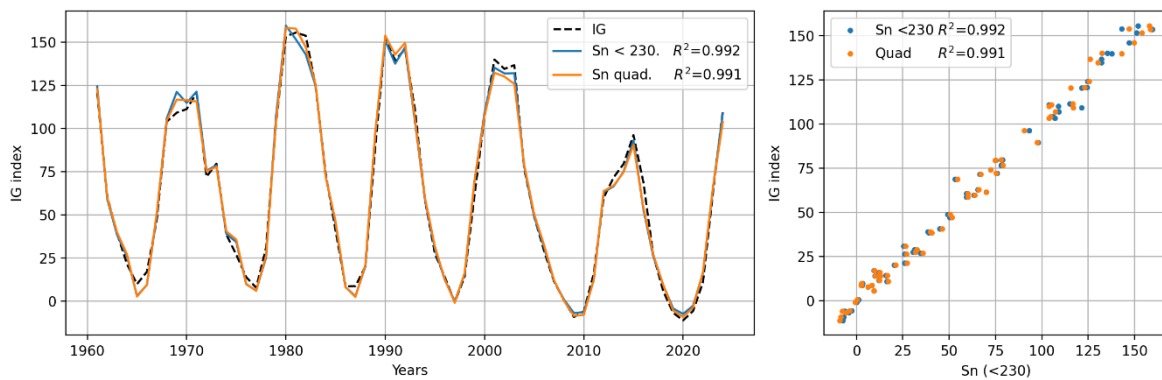


219

220 Figure 5. Linear and quadratic regression between proxies and IG separately for periods 1960-1997
 221 (top panels), and 1985-2023 (bottom panels).

222 Is then the sunspot number the best EUV proxy to model foF2? The evidence up to this point
 223 suggests that is more stable considering longer datasets. The saturation effect could be affecting
 224 the correlation, therefore, subtracting from the daily dataset the Sn higher than 230 (~5% of data)
 225 and calculating the annual mean we obtain an excellent improvement in the linear correlation
 226 between Sn and IG. This method can be also used with F30 and F10.7, but the improvement is not
 227 as good as with the sunspot number (see Table 1). In addition, we model the annual IG using a
 228 quadratic regression; both results can be seen in Figure 6. Since Sn is the only proxy that shows the
 229 down step between cycle 23 and 24 minimums, like IG and most ionospheric stations, it obtains the
 230 highest correlation using the complete period.

231



232

233 Figure 6. IG index (black dashed) and IG index modeled using quadratic regression (orange) and Sn
 234 de-saturated (<230, blue). The right panel shows IG vs IG modeled.

235

236 The correlation using a de-saturated Sn and quadratic regression shows a significant improvement
237 over the original dataset, compared to Sn in Figure 3. The maximums of all cycles after 1970 are
238 close to IG values. Moreover, the last two minimums are much better represented using the
239 quadratic regression and de-saturating the Sn dataset. The squared correlations between indices
240 and stations using quadratic regression can be seen in Table 1, compared to linear and de-saturated
241 Sn. The Table shows that quadratic regression using Sn is, on average, the most effective to predict
242 the ionospheric foF2, followed by Sn de-saturated and quadratic F10.7.

243

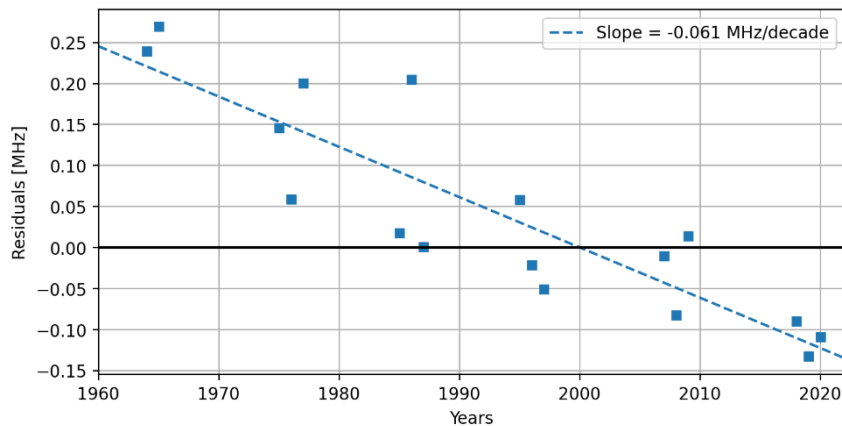
244 Table 1. Squared correlation (R^2) between stations and indices using a quadratic regression over the
245 complete period (1960-2023), compared with linear and de-saturated Sn.

	Sn linear	F30 quad	F10.7 quad	Sn quad	Sn (<230)
Okinawa	0.917	0.859	0.940	0.944	0.939
Wakkanai	0.967	0.968	0.966	0.970	0.968
Kokubunji	0.981	0.979	0.984	0.989	0.988
Townsville	0.947	0.921	0.968	0.972	0.967
Canberra	0.980	0.972	0.983	0.988	0.989
Hobart	0.974	0.975	0.976	0.980	0.980
Juliusruh	0.983	0.981	0.978	0.984	0.981
Rome	0.970	0.971	0.976	0.979	0.978
Boulder	0.953	0.950	0.957	0.962	0.965
Sodankyla	0.911	0.900	0.901	0.911	0.907
Average	0.958	0.947	0.963	0.968	0.966

246

247 The only remaining task is the estimation of the long-term trend using a highly reliable proxy. From
248 Figure 6, we can expect a nearly zero trend for the complete period. This is confirmed by filtering
249 the solar activity from the IG dataset using de-saturated Sn and calculating the residuals, which yield
250 a trend of -0.008 %/decade. However, if we take a close look at the minimum's solar times in Figure
251 6, a clear trend can be noted: IG is higher than Sn in 1965 but lower in 2020. Considering that the
252 CO2 cooling effect over the thermosphere is more pronounced during minimum solar conditions
253 (Emmert et al. 2008, Brown et al. 2024), we could assume a more noticeable effect over the
254 ionospheric parameters as well during lower solar conditions. The theoretical trend estimated using
255 a general circulation model (WACCM-X) is -0.6 %/decade for foF2 (Solomon et al. 2018). Therefore,
256 by focusing on the minimum solar years (1963-1965, 1975-1977, 1985-1987, 1995-1997, 2007-2009,
257 2018-2020), the trend results in -0.79 %/decade, really close to the theoretical value. The residuals
258 from this procedure are shown in Figure 7, where a clear and constant trend is noticed. Is important
259 to note that experimental trend using a similar approach on ionospheric stations data results in

260 much higher values, between 0.04 and 0.21 MHz/decade (Lastovicka 2024; Zossi et al. 2024).
261 Mikhailov et al. (2017) also found a better correlation using the sunspot number over F10.7 in the
262 long-term trend of critical frequency of E-layer.



263

264 Figure 7. Residuals for solar cycle minimums years using Sn de-saturated.

265

266 5. Conclusions

267 In this work, we found that the sunspot number is the most reliable solar EUV proxy for predicting
268 ionospheric index IG over the period 1960-2023. This index is a good indicator of the global
269 ionospheric foF2, as is shown in Figure 1, and supporting by the R^2 value.

270 While many recent articles claim F30 as the superior solar EUV proxy, it fails at representing the step
271 down during the last two solar minimums—a decline that is evident in the Sn dataset. Some of these
272 studies analyze shorter periods in order to use more stations. In Figure 2, we show that F30 is the
273 proxy with better stability to represent each cycle separately. However, analyzing the period 1960-
274 2023, Sn outperforms the F30 correlation, as shown in Figure 3.

275 The main issue with F10.7 and F30 is the last two solar cycle minimums, where the ionospheric foF2
276 decreases more than expected, and a linear model cannot reproduce this decrease using the solar
277 radio fluxes. The sunspot number, on the other hand, effectively handles this issue. When applying
278 a quadratic regression, or neglecting saturation effects from the daily database, Sn obtains the
279 highest correlation, reproducing reliably the last two cycles.

280 The only problem with this methodology is that if we calculate the long-term trend filtering the solar
281 activity, we do not obtain the trend predicted by the global circulation models. Nevertheless, as we
282 point out in Figure 6, minimum solar activity periods have a noticeable trend that results to be in
283 good agreement with the theoretical trend.

284

285 Acknowledgment

286 B.S. Zossi, F.D. Medina, and A.G. Elias acknowledge research projects PIP 2957 and PIUNT E756. T.
287 Duran acknowledges research projects PICT 2019-03491 and PGI 24/F083.

288 Open Research

289 All data used in this work are in public domain. For ionospheric foF2 (1) National Institute of
290 Information and Communications Technology, NICT
291 (https://wdc.nict.go.jp/IONO/HP2009/ISDJ/manual_txt-E.html). (2) The Australian Bureau of
292 Meteorology (<https://downloads.sws.bom.gov.au/wdc/ionodata/au/>). (3) The Lowell GIRO Data
293 Center (<https://giro.uml.edu/didbase/scaled.php>). F10.7 at [https://spaceweather.gc.ca/forecast-](https://spaceweather.gc.ca/forecast-prevision/solar-solaire/solarflux/sx-en.php)
294 [prevision/solar-solaire/solarflux/sx-en.php](https://spaceweather.gc.ca/forecast-prevision/solar-solaire/solarflux/sx-en.php). Sn from the revised Sn database obtained from SILSO
295 (Sunspot Index and Long-term Solar Observations), Royal Observatory of Belgium, at
296 <https://www.sidc.be/SILSO/datafiles>, F30 from the National Astronomical Observatory of Japan at
297 http://solar.nro.nao.ac.jp/norp/html/daily_flux.html.

298

299 References

300 Balan, N., Bailey, G. J., & Moffett, R. J. (1994). Modeling studies of ionospheric variations
301 during an intense solar cycle. *Journal of Geophysical Research: Space Physics*,
302 99(A9), 17467–17475. <https://doi.org/10.1029/94JA01262>

303 Bilitza, D., Pezzopane, M., Truhlik, V., Altadill, D., Reinisch, B. W., & Pignalberi, A.
304 (2022). The International Reference Ionosphere Model: A Review and Description of
305 an Ionospheric Benchmark. *Reviews of Geophysics*, 60(4), e2022RG000792.
306 <https://doi.org/10.1029/2022RG000792>

307 Brown, M. K., Lewis, H. G., Kavanagh, A. J., Cnossen, I., & Elvidge, S. (2024). Future
308 Climate Change in the Thermosphere Under Varying Solar Activity Conditions. *Jour-*
309 *nal of Geophysical Research: Space Physics*, 129(9), e2024JA032659.
310 <https://doi.org/10.1029/2024JA032659>

311 Clette, F. (2021). Is the F10.7cm – Sunspot Number relation linear and stable? *Journal of*
312 *Space Weather and Space Climate*, 11, 2. <https://doi.org/10.1051/SWSC/2020071>

313 Damboldt T, Suessmann P (2012). Consolidated Database of Worldwide Measured
314 Monthly Medians of Ionospheric Characteristics foF2 and M(3000)F2. INAG (Iono-
315 sonde Network Advisory Group) Bulletin 73 [https://www.ursi.org/files/Commission-](https://www.ursi.org/files/Commission-Websites/INAG/web-73/2012/damboldt_consolidated_database.pdf)
316 [Websites/INAG/web-73/2012/damboldt_consolidated_database.pdf](https://www.ursi.org/files/Commission-Websites/INAG/web-73/2012/damboldt_consolidated_database.pdf)

317 Danilov, A. D., Berbeneva, N. A., & Konstantinova, A. V. (2024). Trends in the F2-layer
318 parameters to 2023. *Advances in Space Research*, 73(12), 6054–6065.
319 <https://doi.org/10.1016/J.ASR.2024.03.036>

320 Danilov, A. and Berbeneva, N. (2023). Statistical analysis of the critical frequency foF2 de-
321 pendence on various solar activity indices, *Advances in Space Research*.

322 de Haro Barbás, B. F., Elias, A. G., Venchiarutti, J. V., Fagre, M., Zossi, B. S., Tan Jun, G.,
323 & Medina, F. D. (2021). MgII as a Solar Proxy to Filter F2-Region Ionospheric Pa-
324 rameters. *Pure and Applied Geophysics*, 178(11), 4605–4618.
325 <https://doi.org/10.1007/S00024-021-02884-Y>

- 326 Dudok De Wit, T., & Bruinsma, S. (2017). The 30 cm radio flux as a solar proxy for ther-
327 mosphere density modelling. *Journal of Space Weather and Space Climate*, 7, A9.
328 <https://doi.org/10.1051/SWSC/2017008>
- 329 Emmert, J. T., Picone, J. M., & Meier, R. R. (2008). Thermospheric global average density
330 trends, 1967–2007, derived from orbits of 5000 near-Earth objects. *Geophysical Re-*
331 *search Letters*, 35(5), 5101. <https://doi.org/10.1029/2007GL032809>
- 332 Jakowski, N., Hoque, M. M., & Mielich, J. (2024). Long-term relationships of ionospheric
333 electron density with solar activity. *Journal of Space Weather and Space Climate*, 14,
334 24. <https://doi.org/10.1051/SWSC/2024023>
- 335 Laštovička, J., Mikhailov, A. V., Ulich, T., Bremer, J., Elias, A. G., Ortiz de Adler, N.,
336 Jara, V., Abarca del Rio, R., Foppiano, A. J., Ovalle, E., & Danilov, A. D. (2006).
337 Long-term trends in foF2: A comparison of various methods. *Journal of Atmospheric*
338 *and Solar-Terrestrial Physics*, 68(17), 1854–1870. [https://doi.org/10.1016/J.JA-](https://doi.org/10.1016/J.JA-STP.2006.02.009)
339 [STP.2006.02.009](https://doi.org/10.1016/J.JA-STP.2006.02.009)
- 340 Laštovička, J. (2021). The best solar activity proxy for long-term ionospheric investiga-
341 tions. *Advances in Space Research*, 68(6), 2354–2360.
342 <https://doi.org/10.1016/J.ASR.2021.06.032>
- 343 Laštovička, J. (2023). Progress in investigating long-term trends in the mesosphere, ther-
344 mosphere, and ionosphere. *Atmospheric Chemistry and Physics*, 23(10), 5783–5800.
345 <https://doi.org/10.5194/ACP-23-5783-2023>.
- 346 Laštovička, J. (2024). Dependence of long-term trends in foF2 at middle latitudes on differ-
347 ent solar activity proxies. *Advances in Space Research*.
348 <https://doi.org/10.1016/J.ASR.2023.09.047>.
- 349 Liu, H. L., Foster, B. T., Hagan, M. E., McInerney, J. M., Maute, A., Qian, L., Richmond,
350 A. D., Roble, R. G., Solomon, S. C., Garcia, R. R., Kinnison, D., Marsh, D. R., Smith,
351 A. K., Richter, J., Sassi, F., & Oberheide, J. (2010). Thermosphere extension of the
352 Whole Atmosphere Community Climate Model. *Journal of Geophysical Research:*
353 *Space Physics*, 115(A12), 12302. <https://doi.org/10.1029/2010JA015586>
- 354 Liu, L., Wan, W., Ning, B., Pirog, O., and Kurkin, V. (2006). Solar activity variations of
355 the ionospheric peak electron density, *Journal of Geophysical Research: Space Phys-*
356 *ics*, 111.
- 357 Liu, J. Y., Chen, V. I., & Lin, J. S. (2003). Statistical investigation of the saturation effect
358 in the ionospheric foF2 versus sunspot, solar radio noise, and solar EUV radiation.
359 *Journal of Geophysical Research: Space Physics*, 108(A2), 1067.
360 <https://doi.org/10.1029/2001JA007543>

- 361 Ma, R., Xu, J., Wang, W., & Yuan, W. (2009). Seasonal and latitudinal differences of the
362 saturation effect between ionospheric NmF2 and solar activity indices. *Journal of Ge-*
363 *ophysical Research: Space Physics*, 114(A10), 10303.
364 <https://doi.org/10.1029/2009JA014353>
- 365 Mikhailov, A. V., Perrone, L., & Nusinov, A. A. (2017). A mechanism of midlatitude
366 noontime foE long-term variations inferred from European observations. *Journal of*
367 *Geophysical Research: Space Physics*, 122(4), 4466–4473.
368 <https://doi.org/10.1002/2017JA023909>
- 369 Mielich, J., & Bremer, J. (2013). Long-term trends in the ionospheric F2 region with differ-
370 ent solar activity indices. *Annales Geophysicae*, 31(2), 291–303.
371 <https://doi.org/10.5194/ANGEO-31-291-2013>
- 372 Mursula, K., Qvick, T., Holappa, L., & Asikainen, T. (2022). Magnetic Storms During the
373 Space Age: Occurrence and Relation to Varying Solar Activity. *Journal of Geophysi-*
374 *cal Research: Space Physics*, 127(12), e2022JA030830.
375 <https://doi.org/10.1029/2022JA030830>
- 376 Mursula, K., Pevtsov, A. A., Asikainen, T., Tähtinen, I., & Yeates, A. R. (2024). Transition
377 to a weaker Sun: Changes in the solar atmosphere during the decay of the Modern
378 Maximum. *Astronomy & Astrophysics*, 685, A170. [https://doi.org/10.1051/0004-](https://doi.org/10.1051/0004-6361/202449231)
379 [6361/202449231](https://doi.org/10.1051/0004-6361/202449231)
- 380 Reinisch, B.W., Galkin, I.A., (2011). Global Ionospheric Radio Observatory (GIRO). *Earth*
381 *Planet Sp* 63, 377–381. <https://doi.org/10.5047/eps.2011.03.001>
- 382 Solomon, S. C., Liu, H. L., Marsh, D. R., McInerney, J. M., Qian, L., & Vitt, F. M. (2018).
383 Whole Atmosphere Simulation of Anthropogenic Climate Change. *Geophysical Re-*
384 *search Letters*, 45(3), 1567–1576. <https://doi.org/10.1002/2017GL076950>
- 385 Zolesi, B., & Cander, L. R. (2014). Ionospheric prediction and forecasting. *Ionospheric*
386 *Prediction and Forecasting*, 1–240. <https://doi.org/10.1007/978-3-642-38430-1>
- 387 Zossi, B. S., Medina, F. D., Duran, T., & Elias, A. G. (2024). Selecting the best solar EUV
388 proxy for long-term timescale applications. *Advances in Space Research*.
389 <https://doi.org/10.1016/J.ASR.2024.07.023>

390